Journal of Computers, Mechanical and Management
Journal homepage: www.jcmm.co.in
e-ISSN: 3009-075X
AN PUBLISHING

Volume 4 Issue 4
Article Number: 25223

Activation Energy and Dielectric Properties of Epoxy Nanocomposites with Carbon Nanotubes and Carbon Black

Manindra Trihotri*[1,2] and U. K. Dwivedi[3]

[1]Department of Physics, IcfaiTech, The ICFAI University, Jaipur, Rajasthan, India 302031
[2]Department of Physics, Maulana Azad National Institute of Technology (MANIT), Bhopal, Madhya Pradesh, India 462003
[3]Amity University Rajasthan, Jaipur, Rajasthan, India 303007

Abstract

This study presents a comparative analysis of multiwall carbon nanotube–epoxy (MWCNT–EP) and carbon black–epoxy (CB–EP) nanocomposites to evaluate the influence of filler concentration and frequency on activation energy and dielectric properties. Activation energy was obtained from the slopes of Arrhenius plots ($\ln\sigma$ vs. $1/T$) at 0.5, 5, and 10 kHz. Both composites showed higher activation energy at 0.5 kHz due to long-range charge-carrier hopping, whereas higher frequencies promoted localized transport between adjacent defect sites. Increasing filler concentration further reduced activation energy, reflecting saturation of dangling bonds, lower density of states, and reduced domain boundary potential. Dielectric analysis revealed that CB–EP composites consistently possessed higher dielectric constants than MWCNT–EP composites at equivalent filler loadings, owing to CB's smaller particle size and greater surface area. For both composites, the dielectric constant decreased with increasing frequency, consistent with interfacial polarization effects. These findings clarify how carbonaceous fillers influence the electrical and dielectric behavior of epoxy nanocomposites.

Keywords: Arrhenius Activation Energy; Dielectric Properties; AC Conductivity; Multiwall Carbon Nanotubes; Carbon Black

1. Introduction

Conducting polymer nanostructures are of great interest because their nanoscale dimensions enable high electrical conductivity, short ionic transport paths, large surface area, low mass, high power-to-weight ratio, and mixed electronic–ionic conduction [1–3]. Advanced dielectric materials are critical for capacitors and pulsed-power devices, where high permittivity, low loss, and reliability are required [4]. In polymer nanocomposites, electrical behavior is strongly governed by filler dispersion, interfacial interactions, filler concentration, curing conditions, and percolation phenomena [5–9]. Below the percolation threshold, these systems behave as insulators, while beyond it conductivity increases through tunneling and hopping mechanisms [10–12]. Carbon-based fillers, including carbon black (CB), carbon nanotubes (CNTs), and carbon fibers, are widely used to enhance polymer conductivity. Among these, CB is particularly effective due to its aggregated morphology, which reduces interparticle distance and increases tunneling contacts, thereby enhancing charge transport [8, 13–19]. CNTs, with high aspect ratio and excellent mechanical strength, also provide substantial reinforcement at low concentrations, though their homogeneous dispersion is challenging because of strong van der Waals interactions [20].

*Corresponding Author: Manindra Trihotri (mtrihotri@iujaipur.edu.in)
Received: 25 Jun 2025; Revised: 24 Jul 2025; Accepted: 15 Aug 2025; Published: 31 Aug 2025

DOI: 10.57159/jcmm.4.4.25223.

Electrical transport in CNT–epoxy composites is governed by tube length, alignment, dispersion quality, and curing conditions, and follows a percolation scaling law with a critical concentration and dimensionality-dependent exponent [21, 22]. The temperature dependence of conductivity in polymer nanocomposites typically follows the Arrhenius relation,

$$\sigma = A \exp\left(-\frac{E_a}{k_B T}\right), \tag{1}$$

where A is the pre-exponential factor, E_a the activation energy, k_B Boltzmann's constant, and T absolute temperature [23]. Epoxy-based nanocomposites are particularly attractive because they combine mechanical strength with favorable dielectric response, influenced by space-charge migration, dipolar orientation, and interfacial polarization [5, 24–29]. Although many studies address polymer nanocomposites with carbonaceous fillers, direct comparisons of MWCNT–epoxy (MWCNT–EP) and CB–epoxy (CB–EP) prepared under identical conditions are limited. In particular, the combined influence of filler concentration and frequency on activation energy and dielectric behavior is not yet fully established, despite its importance for optimizing material performance in dielectric and energy-storage applications. The present work addresses this gap by systematically investigating the activation energy, dielectric constant, dissipation factor, and AC conductivity of MWCNT–EP and CB–EP nanocomposites as functions of filler concentration and frequency. The analysis provides insight into the mechanisms by which carbonaceous fillers tailor the electrical and dielectric performance of epoxy-based systems and highlights differences in their effectiveness as reinforcing agents.

2. Materials and Methods

2.1. Materials

Industrial-grade multiwall carbon nanotubes (MWCNTs, 1205YJ, purity >95%) were obtained from Nanostructured & Amorphous Materials, Inc., USA. The nanotubes had an outer diameter of 10–20 nm, inner diameter of 5–10 nm, length of 10–30 μm, specific surface area of 180–230 m^2/g, and bulk density of 0.04–0.05 g/cm^3. Ketjenblack EC-600 JD carbon black (Akzonobel) was used as the second filler, characterized by a BET surface area of 1400 m^2/g, particle diameter of 36 nm, bulk density of 0.12 g/cm^3, iodine absorption of 1000–1100 mg/g, DBP pore volume of 480–510 ml/100 g, and ash content <0.1%. Unmodified epoxy resin (Atul Pvt. Ltd., Valsad, India) served as the polymer matrix, with cured resin density of 1.15 g/cm^3 at room temperature. A standard epoxy-to-hardener ratio of 10:1 was used for all samples.

2.2. Composite Preparation

MWCNT–epoxy (MWCNT–EP) and carbon black–epoxy (CB–EP) composites were prepared by solution casting. For MWCNT–EP, nanotubes were dispersed in epoxy resin preheated to 60 °C and sonicated for 30 min in an ultrasonic bath. The mixture was reheated to reduce viscosity, followed by an additional 30 min of sonication, while minimizing prolonged exposure to prevent nanotube damage. The dispersion was stirred at 200 rpm and 60 °C for 60 min on a hot plate stirrer, cooled to room temperature, and then mixed with hardener to initiate curing. For CB–EP composites, carbon black powder was pre-dried at 60 °C for 30 min to remove moisture. Epoxy resin was heated to 60 °C and mixed with CB to achieve initial dispersion, followed by alternating sonication (30 min), reheating (15 min), and further sonication (30 min). The mixture was stirred at 200 rpm and 50 °C for 60 min, cooled, and then blended with hardener. Vacuum mixing was applied to eliminate entrapped air before casting. Both MWCNT–EP and CB–EP systems were prepared at filler concentrations of 0.5, 1.0, 1.5, 2.0, 2.25, and 2.5 w/v%. The composites were molded into sheets and cured at room temperature for seven days. Square specimens (10 mm × 10 mm × 2 mm) were cut, polished for uniformity, and coated on both sides with conductive silver paint. The solvent was removed by heating the coated samples at 60 °C for 10 min.

2.3. Characterization

Electrical Conductivity and Activation Energy

Electrical conductivity was measured as a function of temperature and frequency. Activation energy was determined using the Arrhenius relation

$$\sigma = A \exp\left(-\frac{E_a}{k_B T}\right), \tag{2}$$

where σ is conductivity, A the pre-exponential factor, E_a the activation energy, k_B Boltzmann's constant, and T absolute temperature. Values of E_a were obtained from the slopes of Arrhenius plots of $\ln \sigma$ versus $1/T$ at different frequencies.

Dielectric Properties

Dielectric measurements were carried out using a Wayne Kerr 6500B impedance analyzer in the frequency range of 500 Hz to 10 kHz. A Wayne Kerr TF-1000 solid sample holder and a high-temperature furnace were employed, with RS-232 and GPIB interfaces enabling computer control. The real (ε') and imaginary (ε'') parts of permittivity were recorded as functions of frequency and temperature. The dielectric constant (ε') was analyzed to assess charge transport and interfacial polarization.

AC Conductivity and Dissipation Factor

AC conductivity (σ_{ac}) was derived from dielectric measurements using the relation

$$\sigma_{ac} = \varepsilon_0 \varepsilon'' \omega,$$

where ε_0 is the permittivity of free space, ε'' the imaginary permittivity, and ω the angular frequency. The dielectric dissipation factor ($\tan\delta$), representing energy loss in the composites, was calculated as the ratio of ε'' to ε'.

3. Results and Discussion

3.1. Activation Energy

Figure 1 shows Arrhenius plots of $\ln(\sigma)$ versus $1/T$ for 0.5 w/v% (a) MWCNT–EP and (b) CB–EP composites at 0.5, 5, and 10 kHz. Activation energies calculated from the slopes are summarized in Tables 1–3. In both composites, E_a decreased with increasing frequency, being highest at 0.5 kHz and lowest at 10 kHz. This trend indicates a transition from phonon-assisted hopping at low frequencies to localized transport between nearest-neighbor defect sites at higher frequencies.

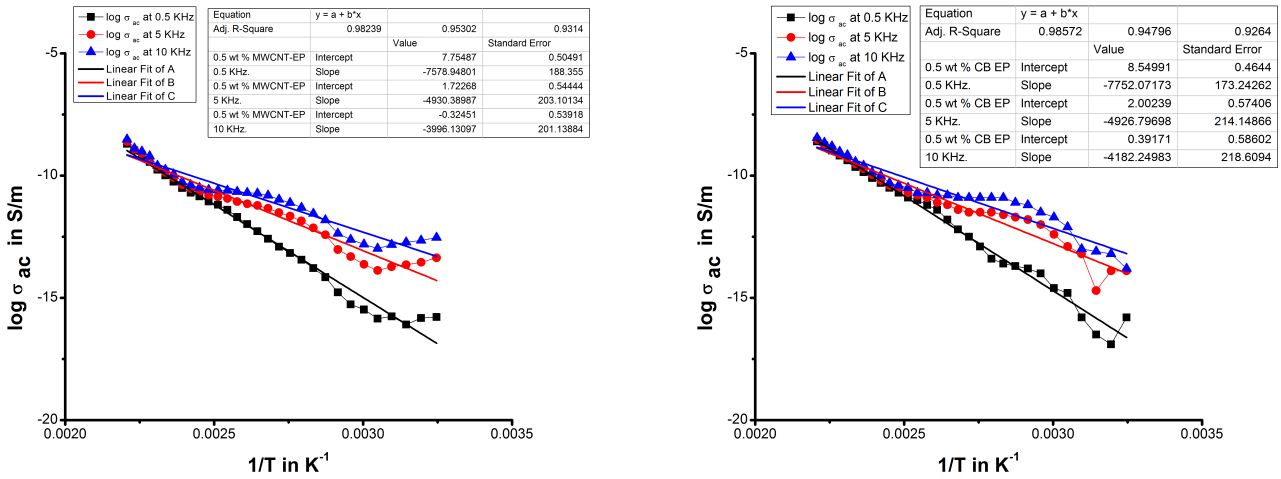

(a) MWCNT–EP composites.

(b) CB–EP composites.

Figure 1: Arrhenius plot of $\ln(\sigma)$ versus $1/T$ for 0.5 w/v% (a) MWCNT–EP and (b) CB–EP composites at 0.5, 5, and 10 kHz.

Table 1: Activation energy (E_a) of MWCNT–EP and CB–EP composites at 0.5 kHz.

Filler (w/v%)	MWCNT–EP (eV)	CB–EP (eV)
0.0	0.6495	0.6495
0.5	0.6530	0.6679
1.0	0.7170	0.6868
1.5	0.6834	0.6727
2.0	0.6548	0.6888
2.5	0.7004	0.5653

Table 2: Activation energy (E_a) of MWCNT–EP and CB–EP composites at 5 kHz.

Filler (w/v%)	MWCNT–EP (eV)	CB–EP (eV)
0.0	0.4693	0.4693
0.5	0.4248	0.4245
1.0	0.4308	0.4534
1.5	0.3987	0.4778
2.0	0.4920	0.4541
2.5	0.3864	0.3680

Table 3: Activation energy (E_a) of MWCNT–EP and CB–EP composites at 10 kHz.

Filler (w/v%)	MWCNT–EP (eV)	CB–EP (eV)
0.0	0.3776	0.3776
0.5	0.3443	0.3603
1.0	0.3335	0.3944
1.5	0.3109	0.4221
2.0	0.4430	0.3672
2.5	0.3252	0.3520

Figure 2 illustrates the effect of filler concentration on activation energy (E_a) at different frequencies. In MWCNT–EP composites, E_a increased slightly with loading at 0.5 kHz [Figure 2(a)] but decreased with loading at higher frequencies [Figures 2(b) and 2(c)]. CB–EP composites, in contrast, showed a consistent decrease in E_a with increasing filler concentration at all frequencies. The lower activation energies in CB–EP systems are attributed to smaller particle size and larger surface area of CB, which enhance dispersion and tunneling efficiency. In MWCNT–EP composites, agglomeration at higher concentrations hinders uniform dispersion and elevates E_a, especially at low frequencies.

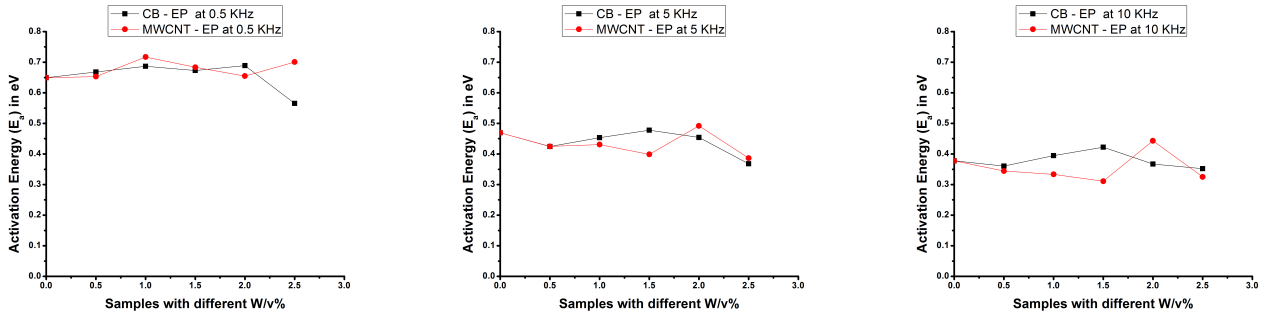

(a) 0.5 kHz **(b)** 5 kHz **(c)** 10 kHz

Figure 2: Effect of filler concentration on activation energy (E_a) in (a) 0.5 kHz, (b) 5 kHz, and (c) 10 kHz.

3.2. Dielectric Constant (ε')

Figure 3 shows the variation of dielectric constant with frequency and filler concentration for both MWCNT–EP and CB–EP composites. In both systems, ε' decreased with increasing frequency from 0.5 to 10 kHz due to the inability of dipoles and interfacial charges to follow the rapid field oscillations. At low frequencies, interfacial polarization dominates because of charge accumulation at filler–matrix boundaries. In MWCNT–EP composites [Figure 3(a)], ε' increased with filler loading, rising from 6.266 to 8.453 at 0.5 kHz and from 5.574 to 7.734 at 10 kHz as concentration increased from 0.5 to 2 w/v%. The improvement is attributed to the high aspect ratio of MWCNTs, which facilitates network formation. In CB–EP composites [Figure 3(b)], dielectric constants were consistently higher, increasing from 6.023 to 9.844 at 0.5 kHz and from 5.546 to 9.266 at 10 kHz. The finer particle size and larger surface area of CB produce stronger Maxwell–Wagner–Sillars polarization, explaining the superior dielectric performance.

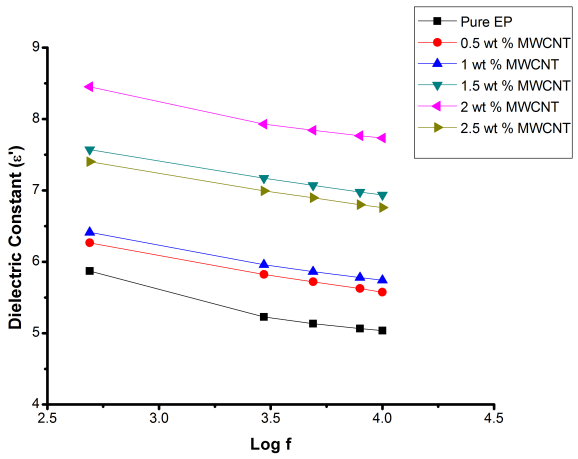

(a) MWCNT–EP composites at different filler concentrations.

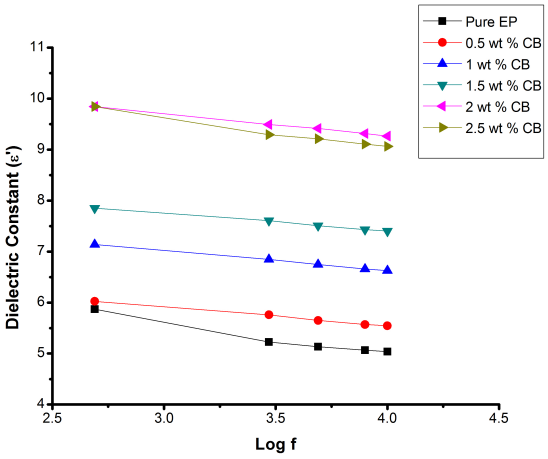

(b) CB–EP composites at different filler concentrations.

Figure 3: Variation of dielectric constant (ε') with $\log f$ for (a) MWCNT–EP and (b) CB–EP composites.

3.3. Dielectric Dissipation Factor (tan δ)

Figure 4 shows the variation of dielectric dissipation factor (tan δ) with frequency for (a) MWCNT–EP and (b) CB–EP composites at different filler concentrations. In both composites, tan δ decreased with increasing frequency but increased with filler loading. For MWCNT–EP composites [Figure 4(a)], values rose from 0.358 at 0.5 w/v% to 0.506 at 2 w/v% (0.5 kHz). For CB–EP composites [Figure 4(b)], the increase was smaller, from 0.312 to 0.350 over the same range. The rise in tan δ with concentration is attributed to enhanced interfacial polarization and charge-carrier density, while aggregation at high loadings reduces homogeneity and moderates loss growth.

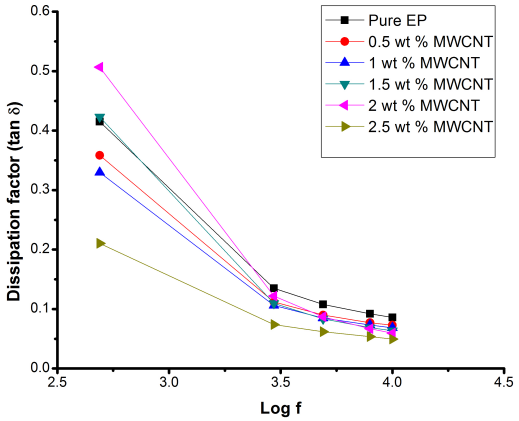

(a) MWCNT–EP composites.

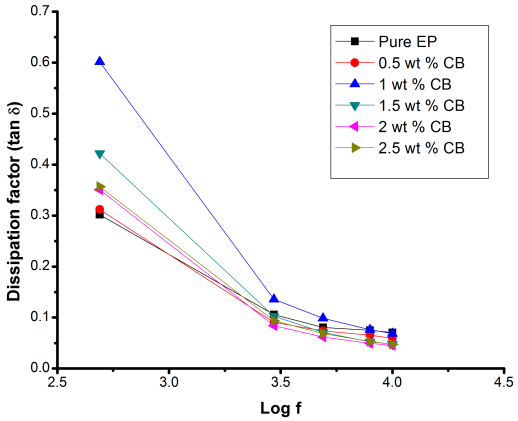

(b) CB–EP composites.

Figure 4: Variation of dielectric dissipation factor (tan δ) with $\log f$ for (a) MWCNT–EP and (b) CB–EP composites at different filler concentrations.

3.4. AC Conductivity (σ_{ac})

Figure 5 illustrates the frequency dependence of AC conductivity for (a) MWCNT–EP and (b) CB–EP composites at different filler concentrations. In both systems, σ_{ac} increased with filler concentration and frequency, consistent with improved charge transport. For MWCNT–EP composites [Figure 5(a)], conductivity rose sharply beyond 3 kHz, signifying the development of percolated conductive networks. At low concentrations, incomplete networks restricted conduction, while higher loadings enabled continuous pathways. Very high concentrations, however, promoted agglomeration, which disrupted network uniformity. For CB–EP composites [Figure 5(b)], conductivity improved steadily with concentration and frequency. At low filler levels, transport occurred mainly by electron hopping between localized sites, while at higher loadings percolation dominated. The frequency dependence followed a power-law trend, reflecting phonon-assisted hopping and interfacial polarization. These results align with the dielectric response and confirm that filler type and concentration strongly influence transport mechanisms in epoxy nanocomposites.

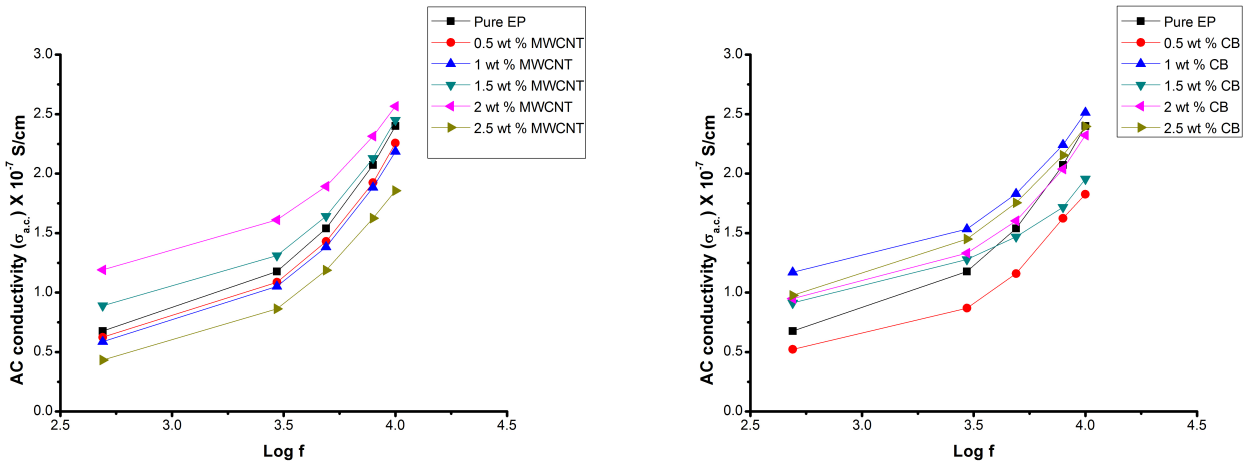

(a) MWCNT–EP composites.

(b) CB–EP composites.

Figure 5: Variation of AC conductivity (σ_{ac}) with $\log f$ for (a) MWCNT–EP and (b) CB–EP composites at different filler concentrations.

4. Conclusions

A comparative analysis of multiwall carbon nanotube–epoxy (MWCNT–EP) and carbon black–epoxy (CB–EP) composites was conducted to evaluate the effect of filler concentration and frequency on Arrhenius activation energy and dielectric properties. The activation energy of both composites was higher at 0.5 kHz than at 5 or 10 kHz. At 0.5 kHz, CB–EP composites exhibited lower activation energies than MWCNT–EP composites, attributed to the smaller particle size and larger surface area of CB, which facilitate charge transport. The dielectric constant at a given frequency was inversely related to activation energy, reflecting the influence of relaxation dynamics. CB–EP composites consistently showed higher dielectric constants than MWCNT–EP composites across all filler concentrations and frequencies, confirming superior interfacial polarization due to finer dispersion. Overall, filler concentration and frequency influence activation energy and dielectric constant primarily through filler type, polymer compatibility, and dispersion quality. These results highlight the importance of optimizing filler selection and loading for tailoring polymer nanocomposites toward specific dielectric applications.

Acknowledgment

The authors are thankful to Prof. Dr. H. P. Singh, President, The ICFAI University, Jaipur-302031 India for support and motivation and acknowledges the support of Dr. S.S. Jain & Dr. A.K. Saini Dean IcfaiTech, The ICFAI University, Jaipur-302031(Rajasthan) India.

Declaration of Competing Interests

The authors declare no known competing financial interests or personal relationships.

Funding Declaration

This research did not receive any specific grant from funding agencies in the public, commercial, or not-for-profit sectors.

Author Contributions

Manindra Trihotri: Conceptualization, Methodology, Experimental Investigation, Data Curation, Formal Analysis, Writing – Original Draft, Writing – Review and Editing, Supervision; **U. K. Dwivedi**: Validation, Resources, Data Interpretation, Visualization, Writing – Review and Editing.

References

[1] J. J. Karippal, H. N. Murthy, K. Rai, M. Krishna, and M. Sreejith, "The processing and characterization of MWCNT/epoxy and CB/epoxy nanocomposites using twin screw extrusion," *Polymer-Plastics Technology and Engineering*, vol. 49, pp. 1207–1213, 2010.

[2] R. J. Tseng, J. Huang, J. Ouyang, R. B. Kaner, and Y. Yang, "Polyaniline nanofiber/gold nanoparticle nonvolatile memory," *Nano Letters*, vol. 5, pp. 1077–1080, 2005.

[3] L. Pan, H. Qiu, C. Dou, Y. Li, L. Pu, J. Xu, and Y. Shi, "Conducting polymer nanostructures: Template synthesis and applications in energy storage," *International Journal of Molecular Sciences*, vol. 11, pp. 2636–2657, 2010.

[4] X. Huang, X. Zhang, G.-K. Ren, J. Jiang, Z. Dan, Q. Zhang, X. Zhang, C.-W. Nan, and Y. Shen, "Non-intuitive concomitant enhancement of dielectric permittivity, breakdown strength and energy density in percolative polymer nanocomposites by trace Ag nanodots," *Journal of Materials Chemistry A*, vol. 7, pp. 15198–15206, 2019.

[5] M. E. Hasnaoui, M. Graça, M. Achour, L. Costa, F. Lahjomri, A. Outzourhit, and A. Oueriagli, "Electrical properties of carbon black/copolymer composites above and below the melting temperature," *Journal of Materials and Environmental Science*, vol. 2, pp. 1–6, 2011.

[6] W. Zhang, R. S. Blackburn, and A. Dehghani-Sanij, "Electrical conductivity of epoxy resin–carbon black–silica nanocomposites: Effect of silica concentration and analysis of polymer curing reaction by FTIR," *Scripta Materialia*, vol. 57, pp. 949–952, 2007.

[7] Q. Liang, M. T. Nyugen, K.-S. Moon, K. Watkins, L. T. Morato, and C. P. Wong, "A kinetics study on electrical resistivity transition of in situ polymer aging sensors based on carbon-black-filled epoxy conductive polymeric composites (CPCs)," *Journal of Electronic Materials*, vol. 42, pp. 1114–1121, 2013.

[8] C. Brosseau, P. Qu'eff'elec, and P. Talbot, "Microwave characterization of filled polymers," *Journal of Applied Physics*, vol. 89, pp. 4532–4540, 2001.

[9] M. E. Hasnaoui, A. Triki, M. Graça, M. Achour, L. Costa, and M. Arous, "Electrical conductivity studies on carbon black loaded ethylene butylacrylate polymer composites," *Journal of Non-Crystalline Solids*, vol. 358, pp. 2810–2815, 2012.

[10] J. Vilč'akov'a, P. Šaha, V. Křes'alek, and O. Quadrat, "Pre-exponential factor and activation energy of electrical conductivity in polyester resin/carbon fibre composites," *Synthetic Metals*, vol. 113, pp. 83–87, 2000.

[11] M. Trihotri, U. Dwivedi, F. H. Khan, M. Malik, and M. Qureshi, "Effect of curing on activation energy and dielectric properties of carbon black–epoxy composites at different temperatures," *Journal of Non-Crystalline Solids*, vol. 421, pp. 1–13, 2015.

[12] A. Avdonin, P. Skupi'nski, and K. Grasza, "Experimental investigation of the typical activation energy and distance of hopping electron transport in ZnO," *Physica B: Condensed Matter*, vol. 562, pp. 94–99, 2019.

[13] J. A. R. Adriaanse, P. A. A. Teunissen, H. B. Brom, M. A. J. Michels, and J. C. M. Brokken-Zijp, "High-dilution carbon-black/polymer composites: Hierarchical percolating network derived from Hz to THz AC conductivity," *Physical Review Letters*, vol. 78, p. 1755, 1997.

[14] J. Yang and L. Li, "Aggregate structure and percolation behavior in polymer/carbon black conductive composites," *Journal of Applied Physics*, vol. 102, p. 083508, 2007.

[15] C. Rubinger, V. Junqueira, G. Ribeiro, and R. Rubinger, "Hopping conduction on conductive inks for wearable electronics," *Journal of Materials Science: Materials in Electronics*, vol. 24, pp. 2091–2097, 2013.

[16] P. K. J. Macutkevic, A. Paddubskaya, S. Maksimenko, J. Banys, A. Celzard, V. Fierro, S. Bistarelli, A. Cataldo, F. Micciulla, and S. Bellucci, "Electrical transport in carbon black–epoxy resin composites at different temperatures," *Journal of Applied Physics*, vol. 114, p. 033707, 2013.

[17] W. S. Chin and D. G. Lee, "Dielectric characteristics of E-glass–polyester composite containing conductive carbon black powder," *Journal of Composite Materials*, vol. 41, pp. 403–417, 2007.

[18] O. G. Abdullah, G. M. Jamal, D. A. Tahir, and S. R. Saeed, "Electrical characterization of polyester reinforced by carbon black particles," *International Journal of Applied Physics and Mathematics*, vol. 1, p. 101, 2011.

[19] Z. Elimat, "AC-impedance and dielectric properties of hybrid polymer composites," *Journal of Composite Materials*, vol. 49, pp. 3–15, 2015.

[20] L. Bokobza, "Multiwall carbon nanotube elastomeric composites: A review," *Polymer*, vol. 48, pp. 4907–4920, 2007.

[21] L. Guadagno, B. D. Vivo, A. D. Bartolomeo, P. Lamberti, A. Sorrentino, V. Tucci, L. Vertuccio, and V. Vittoria, "Effect of functionalization on the thermo-mechanical and electrical behavior of multi-wall carbon nanotube/epoxy composites," *Carbon*, vol. 49, pp. 1919–1930, 2011.

[22] M. Trihotri, U. Dwivedi, M. Malik, F. H. Khan, and M. Qureshi, "Study of low weight percentage filler on dielectric properties of MCWNT-epoxy nanocomposites," *Journal of Advanced Dielectrics*, vol. 6, p. 1650024, 2016.

[23] L. Sudha, R. Sukumar, and K. U. Rao, "Evaluation of activation energy (e_a) profiles of nanostructured alumina polycarbonate composite insulation materials," *International Journal of Materials, Mechanics and Manufacturing*, vol. 2, pp. 96–100, 2014.

[24] J. Katayama, Y. Ohki, N. Fuse, M. Kozako, and T. Tanaka, "Effects of nanofiller materials on the dielectric properties of epoxy nanocomposites," *IEEE Transactions on Dielectrics and Electrical Insulation*, vol. 20, pp. 157–165, 2013.

[25] Q. Wang and G. Chen, "Effect of nanofillers on the dielectric properties of epoxy nanocomposites," *Advances in Materials Research*, vol. 1, pp. 93–107, 2012.

[26] M. Achour, A. Mdarhri, F. Carmona, F. Lahjomri, and A. Oueriagli, "Dielectric properties of carbon black–epoxy resin composites studied with impedance spectroscopy," *Spectroscopy Letters*, vol. 41, pp. 81–86, 2008.

[27] R. Strumpler and J. Glatz-Reichenbach, "Conducting polymer composites," *Journal of Electroceramics*, vol. 3, pp. 329–346, 1999.

[28] J. P. Runt and J. J. Fitzgerald, *Dielectric Spectroscopy of Polymeric Materials*. American Chemical Society, 1997.

[29] N. Singh, S. Shah, A. Qureshi, A. Tripathi, F. Singh, D. Avasthi, and P. Raole, "Effect of ion beam irradiation on metal particle doped polymer composites," *Bulletin of Materials Science*, vol. 34, pp. 81–88, 2011.